

Morphological, Structural and Optical Properties Study of Transition Metal Ions Doped TiO₂ Nanotubes Prepared by Hydrothermal Method

Mohd Hasmizam Razali, Ahmad-Fauzi M. N., Abdul Rahman Mohamed, and Srimala Sreekantan

Abstract—Undoped TiO₂ nanotubes and doped titanium dioxide nanotubes with various transition metal ions (Co²⁺, Ni²⁺, Cu²⁺) were prepared by hydrothermal method. The samples were characterized using X-ray diffraction (XRD), field-emission scanning electron microscopy (FESEM), transmission electron microscopy (TEM), nitrogen gas adsorption and UV-Vis diffuse reflectance spectroscopy. The structural and morphological studies showed that the transition metal ion dopant was incorporated into interstitial positions of the TiO₂ lattice to form a new phase of TiO₂ (hexagonal) instead of anatase TiO₂ (tetragonal) for undoped TiO₂ nanotubes. It could be expected that doped TiO₂ nanotubes active under visible light due to their small band gap.

Index Terms—Doped, photocatalyst, TiO₂ nanotubes, transition metal ion.

I. INTRODUCTION

Recently, extensive researches have been conducted on the synthesis and characterization of TiO₂ nanotubes because of their novel properties such as unique shape, size confinement in radial-direction, large specific surface area and large pores volumes [1]. They also have high interfacial charge transfer rate, resulting in the carriers being free to move throughout the length of these nanostructures thus, reduce the e⁻/h⁺ recombination probability [2]. However, due to their large band gap energy (~ 3.25 eV) [3], it is only active only under UV-light spectral range, which is a small fraction (5–6) % of whole solar-light spectrum [4], [5]. Therefore, doped titanium dioxide nanotubes photocatalyst have been extensively investigated due to their capability to extend the wavelength response of TiO₂ nanotubes into the visible region and inhibits phase transformation. Moreover, doping could enhance its photoactivity by reducing the recombination of e⁻ and h⁺ pair and enhancing the interfacial

charge transfer [6], [7]. So far, various transition metal ions [8], [9], noble metal [10], and non-metals [11]–[13] doped TiO₂ have been successfully prepared and investigated. However, there is a considerable controversy on the effect of doping metal-ions on photocatalytic performance. Some papers reported that the doping of metal-ions such as W⁶⁺ and Cu²⁺ in TiO₂ increased the photocatalytic performance [14], [15], whereas Nagaveni *et al.*, demonstrated that TiO₂ doping with these metal-ions through solution combustion method showed weaker photocatalytic performance than pure TiO₂ [16]. Such wide variations in reported literatures should be mainly due to different preparation methods and doping elements which resulted in different physical properties of TiO₂. Thus, in this present work, various transition metal ions doped TiO₂ nanotubes were synthesized by hydrothermal method and were characterized using FESEM, TEM, XRD, nitrogen gas sorption and UV-Vis diffuse reflectance spectroscopy.

II. EXPERIMENTAL

A. Preparation of Undoped and Doped TiO₂ Nanotubes

To synthesize undoped TiO₂ nanotube, 2 g of the commercial TiO₂ powder precursor (merck) was mixed with 100 mL of 10 M NaOH. The mixture was subjected to hydrothermal treatment at 150 °C for 24 hours in autoclave. When the reaction was completed, the white solid was collected and washed with 0.1 M HCl (200 mL) followed by distilled water until a pH 7 of washing solution was obtained. The final products were obtained by the filtration with subsequent drying at 80 °C for 24 hours. Then, sample was heated at 300 °C for 2 hours in the air. In order to synthesize Co²⁺, Ni²⁺ and Cu²⁺ doped nanotubes, similar procedure was repeated with 2 g of TiO₂ precursor was mixed with 100 mL of 10 M NaOH consists of 0.25 mmol of Co(NO₃)₂, Ni(NO₃)₂ and Cu(NO₃)₂ aqueous solution as metal ions source respectively.

B. Characterization

ZEISS SUPRATM 35VP field emission scanning electron microscope (FESEM) and Philips CM12 transmission electron microscope (TEM) was used to investigate the morphology of the sample. X-Ray powder diffraction (XRD) analysis was performed using a Bruker D8 Diffractometer with Cu-K α (λ = 1.54021 Å) and scans were performed in step of 0.2°/second over the range of 2 θ from 10 up to 80°. Quantachrome ASiQwin - nitrogen gas adsorption was used to determine the surface area and UV-Vis was carried out

Manuscript received January 14, 2013; revised March 16, 2013.

This work was supported by the USM PRGS. Morphological, structural and optical properties study of transition metal ions doped TiO₂ nanotubes prepared by hydrothermal method.

Mohd Hasmizam Razali is with the Department of Chemical Sciences, Faculty of Science and Technology, Universiti Malaysia Terengganu, 21310 Kuala Terengganu, Terengganu, Malaysia (e-mail: mdhasmizam@umt.edu.my).

Ahmad-Fauzi M. N. and Srimala Sreekantan are with the School of Material and Mineral Resources Engineering, Universiti Sains Malaysia, Engineering Campus, Seri Ampangan, 14300 USM, Nibong Tebal, Pulau Pinang, Malaysia (e-mail: afauzi@eng.usm.my, srimala@eng.usm.my).

Abdul Rahman Mohamed is with the School of Chemical Engineering, Universiti Sains Malaysia, Engineering Campus, Seri Ampangan, 14300 USM, Nibong Tebal, Pulau Pinang, Malaysia (e-mail: chrahman@eng.usm.my).

using Perkin Elmer Lambda UV-Vis spectrometer for band gap measurements.

III. RESULT AND DISCUSSION

The XRD patterns of undoped TiO₂ nanotubes and doped TiO₂ nanotubes with different metal ion shown in Fig. 1. TiO₂ nanotubes revealed the presence of the peaks at 25.25°, 37.52°, 48.02°, 53.58°, 54.88°, 62.61°, and 75.07° which are assigned to TiO₂ anatase. Meanwhile for Co²⁺, Ni²⁺, Cu²⁺ doped TiO₂ nanotubes at 0.25 mmol, only three peaks at about 19.89°, 24.57° and 48.30° was observed. These peaks were due to the hexagonal phase of TiO₂.

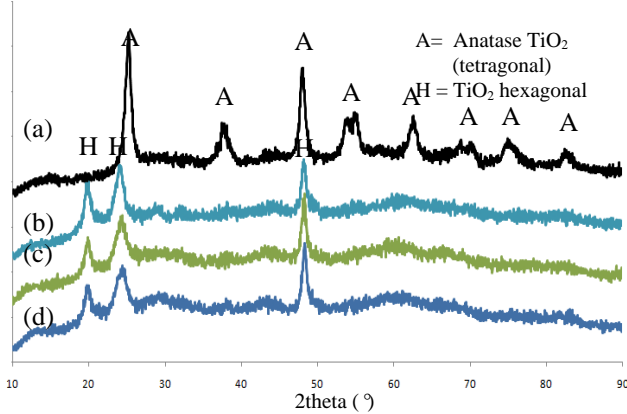


Fig. 1. XRD patterns of (a) undoped TiO₂ nanotubes and 0.25 mmol doped TiO₂ nanotubes with (b) Co²⁺ (c) Ni²⁺ (d) Cu²⁺ metal ion

The lattice parameters of TiO₂ nanotubes and various transition metal ion doped TiO₂ nanotubes based on the XRD patterns are listed in Table I.

TABLE I: LATTICE PARAMETERS AND PHASE CONTENT OF THE SAMPLES

Sample	<i>a</i> (Å)	<i>c</i> (Å)	Phase content (%)
TiO ₂ nanotubes	3.781	9.509	100 anatase TiO ₂
Co ²⁺ doped TiO ₂ nanotubes	5.05	6.51	100 TiO ₂ hexagonal
Ni ²⁺ doped TiO ₂ nanotubes	5.11	6.45	100 TiO ₂ hexagonal
Cu ²⁺ doped TiO ₂ nanotubes	5.12	6.38	100 TiO ₂ hexagonal
Anatase TiO ₂ (tetragonal)	3.784	9.519	-
TiO ₂ hexagonal	5.29	6.13	-

It can be seen that TiO₂ nanotubes have lattice parameters (*a*- and *c*-axis) of 3.781 Å and 9.509 Å, respectively, in the unit cell based on the tetragonal Bravais lattice. In comparison with doped titania nanotubes, there exists derivations of *a* and *c* values. This derivation as well as formation of new phase after metal ion doping is most probably due to the incorporation of metal ion into interstitial positions of the TiO₂ lattice. The interstitial diffusion of metal ion into the TiO₂ lattice can strongly modify the lattice parameters. In addition, no additional peaks corresponding to the dopants were observed proving those dopants ions are successfully incorporated into the lattice site of TiO₂. However, researchers [17], [18] reported that no peaks of dopant were observed in XRD pattern due to low concentration of dopant loading into TiO₂ nanotubes. The

XRD cannot identify the dopant peaks because of their detection limit.

In order to study the effect of transition metal ion doping on morphology of nanotubes, the FESEM and TEM was carried out. Fig. 2 represents the FESEM micrographs of undoped TiO₂ nanotubes and doped TiO₂ nanotubes with different metal ions (Co²⁺, Ni²⁺, Cu²⁺). Fibrous-like structures is shown by FESEM image for undoped TiO₂ nanotubes (Fig. 2a). The diameter of the fibrous is about 12 nm. On the other hand, after doping with different metal ion of Ni²⁺ (Fig. 2b), Co²⁺ (Fig. 2c) and Cu²⁺ (Fig. 2d), similar morphological characteristics was observed. This indicating that, the metal ion doping had little effect on fibrous-like structure may be due to small amount of metal ion loading.

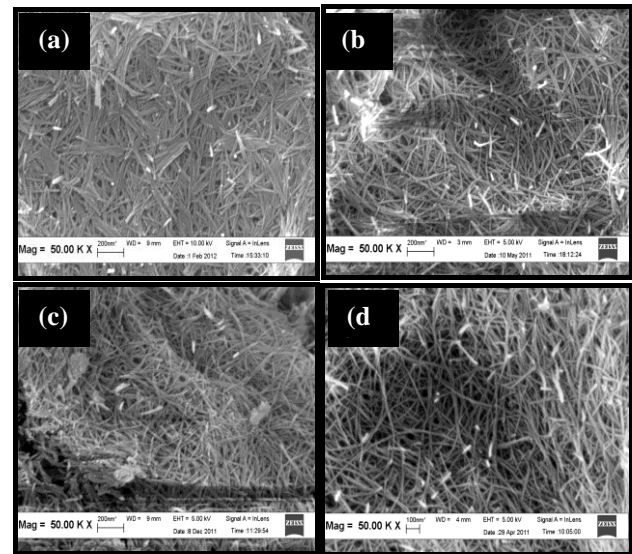


Fig. 2. FESEM micrographs of (a) undoped TiO₂ nanotubes, and 0.25 mmol doped TiO₂ nanotubes with (b) Co²⁺ (c) Ni²⁺ (d) Cu²⁺ metal ion

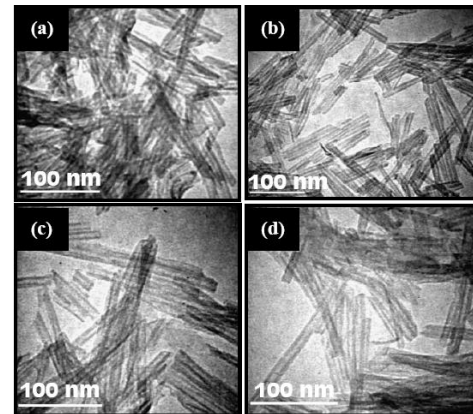


Fig. 3. TEM micrographs of (a) undoped TiO₂ nanotubes and 0.25 mmol doped TiO₂ nanotubes with (b) Co²⁺ (c) Ni²⁺ (d) Cu²⁺ metal ion

Meanwhile, TEM micrographs of the undoped and doped TiO₂ nanotubes are shown in Fig. 3. Fig. 3a shows TEM images of the undoped TiO₂ nanotubes. The existence of hollow inside the fibrous-like structures indicated for nanotubes formation. The inner and outer diameters of the nanotubes are 4 nm and 12 nm respectively. After doping with metal ion, there were no obvious changes in their morphological structure. All doped TiO₂ nanotubes also showed the existence of hollow inside the fibrous-like structure indicating that nanotubes structures were retained (Fig. 3b, 3c, 3d). The nanotubes structures were connected

randomly. This will promotes the diffusion of reactants and products, thus enhancing the photocatalytic activity by facilitating access to the reactive sites on the surface of the photocatalyst [19]. In addition, photocatalytic reactions are believed to take place on the illuminated surface. The tube-like structure increases the surface areas significantly and, consequently, helps rapid mass transfer of the adsorbed molecules from bulk solution onto the catalyst surface, causing the photocatalytic process to be accelerated [20].

TABLE II: BET SURFACE AREA OF TiO_2 PRECURSOR, UNDOPED TiO_2 NANOTUBES AND DOPED TiO_2 NANOTUBES

Samples	BET surface area (m^2/g)
TiO_2 precursor	9.280
Undoped TiO_2 nanotubes	226.521
Co^{2+} doped TiO_2 nanotubes	240.441
Ni^{2+} doped TiO_2 nanotubes	242.262
Cu^{2+} doped TiO_2 nanotubes	245.075

As shown in Table II the BET surface area of the TiO_2 precursor is $9.280 \text{ m}^2/\text{g}$. However for undoped TiO_2 nanotubes, the value increases drastically to $226.521 \text{ m}^2/\text{g}$. It is predicted that the inner and outer surfaces of tubes structure are the major reason for the increase in surface area, which was one of the new attribute of the TiO_2 nanotubes compared with TiO_2 precursor. On the other hand, the BET surface areas of doped TiO_2 nanotubes are larger than undoped TiO_2 nanotubes due to the presence of dopant, which can reduced TiO_2 crystallization and grain growth during the heat decomposition step, thus producing larger surface area material [21]. For doped material, the trends show that the BET surface area increases from $240.441 \text{ m}^2/\text{g}$ to $241.262 \text{ m}^2/\text{g}$ and $245.075 \text{ m}^2/\text{g}$ upon the addition of transition metal ion series from left to right of the periodic table (Co^{2+} , Ni^{2+} , Cu^{2+}). The differential of transition metal ion size may be contributed to the deviation of surface area.

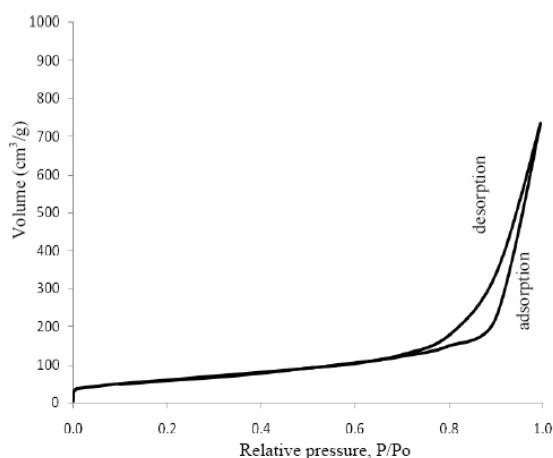


Fig. 4. Isotherm plot of undoped TiO_2 nanotubes

Fig. 4-7 shows the N_2 adsorption-desorption isotherms of undoped TiO_2 nanotube and doped TiO_2 nanotubes. The isotherm for all samples exhibits a typical IV-like isotherm with H1 hysteresis according to IUPAC classification [22]. The shapes of hysteresis loops have often been identified

with specific pore structures. Type H1 hysteresis appearing in the multilayer range of physisorption isotherms is usually associated with capillary condensation in mesopore structures. Mesoporous structures allowed rapid diffusion of various reactants and product molecules passing through the pores during photodegradation reaction [22].

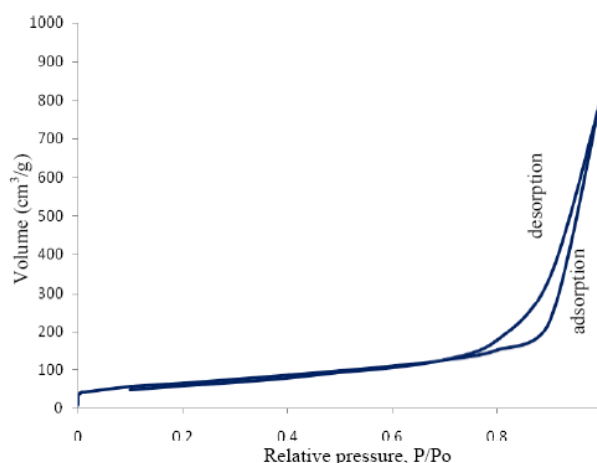


Fig. 5. Isotherm plot of $0.25 \text{ mmol Co}^{2+}$ doped TiO_2 nanotubes

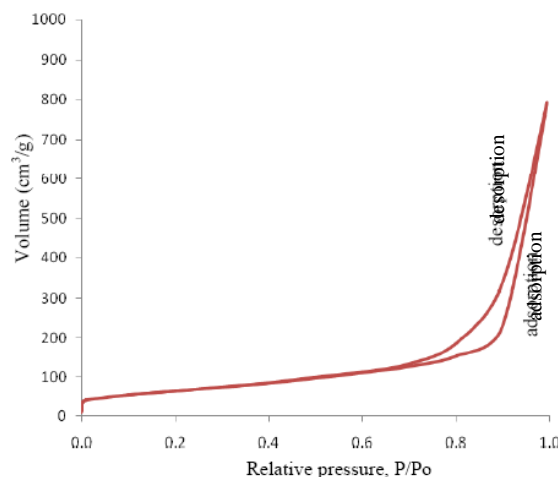


Fig. 6. Isotherm plot of $0.25 \text{ mmol Ni}^{2+}$ doped TiO_2 nanotubes

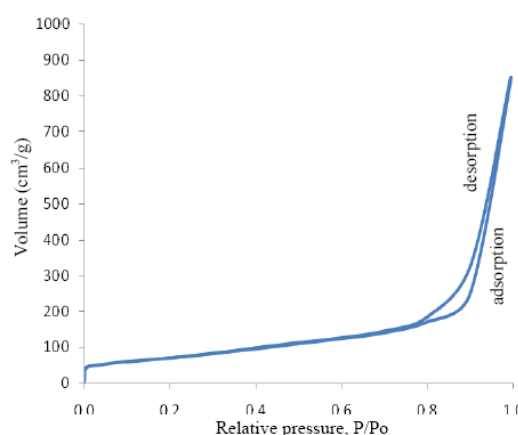


Fig. 7. Isotherm plot of $0.025 \text{ mmol Co}^{2+}$ doped TiO_2 nanotubes

The band gap energy of the undoped titania nanotubes and doped nanotubes (copper ion) were determined from the reflectance data obtained in reflectance spectra [Fig. 8 and 10]. A graph of $[\ln(R_{\text{max}} - R_{\text{min}}/R - R_{\text{min}})]^2$ versus photon energy

(band gap energy) was plotted, where R_{\max} represents the maximum reflectance value in desired wavelength and R_{\min} represents the minimum reflectance value in desired wavelength. The energy band gap was determined based on the intersection from the extrapolation of the straight line of the curve to the y-axis = 0 [23]. In this study, the band gap energy of the undoped TiO_2 nanotubes is about ~ 3.27 eV (Fig. 9). The doped titanium dioxide nanotubes (with copper ion) on the other hand, show very small in their band gap energy (~ 2.06 eV) (Fig. 11), and shifted to the blue region wavelength in reflectance spectra. This probably due to the formation of a new phase (hexagonal) of TiO_2

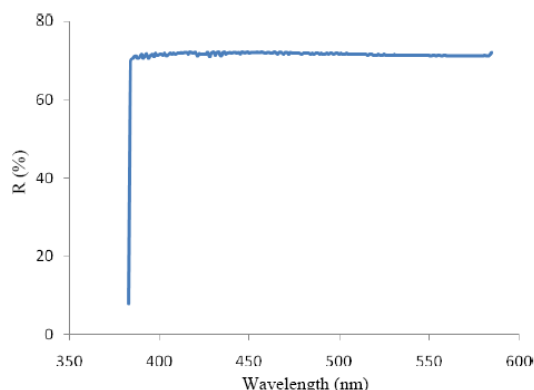


Fig. 8. Reflectance spectra of undoped TiO_2 nanotubes

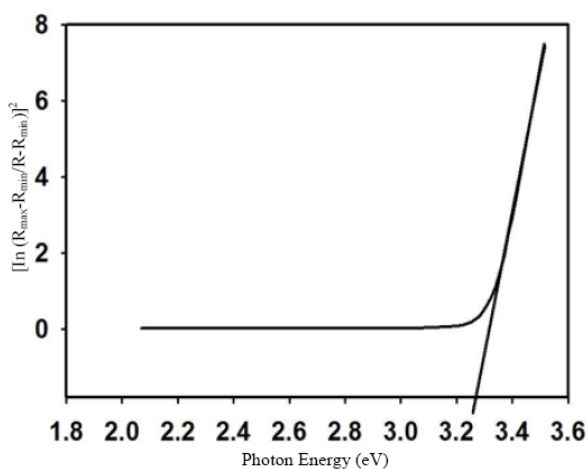


Fig 9. Energy band gap of undoped TiO_2 nanotubes

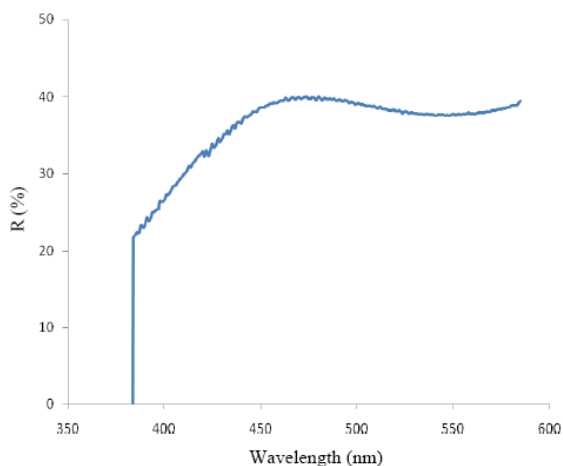


Fig. 10. Reflectance spectra of copper ion doped TiO_2 nanotubes

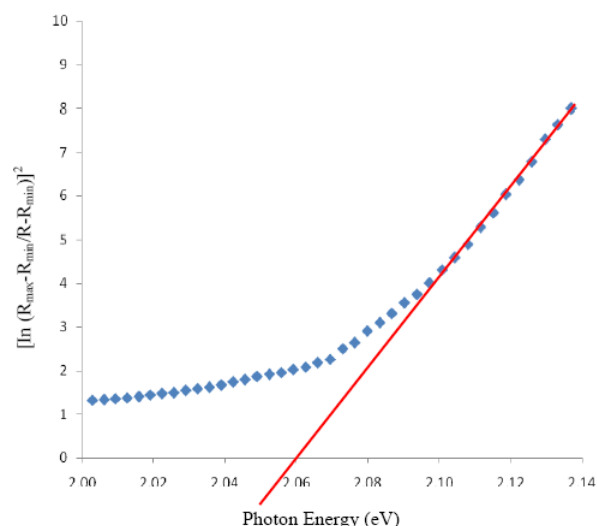


Fig. 11. Energy band gap of copper ion doped TiO_2 nanotubes

ACKNOWLEDGMENT

We are grateful to Universiti Sains Malaysia (USM) for providing the facilities to carry out this project. We would also like to thank Universiti Malaysia Terengganu (UMT) and Ministry of Higher Education of Malaysia (MOHE) for financial support.

REFERENCES

- [1] J. Yu, H. Yu, B. Cheng, and C. Trapalis, "Effects of calcination temperature on the microstructures and photocatalytic activity of titanate nanotubes," *J. Mol. Catal. A: Chem.*, vol. 249, pp. 135–142, 2006.
- [2] C. Juan Carlos, L. Rafael, C. Juan Manuel, C. Fernando, K. Zbigniew, and R. Antonio Angel, "Nanostructured Photocatalysts and Their Applications in the Photocatalytic Transformation of Lignocellulosic Biomass: An Overview," *Materials*, vol. 2, pp. 2228–2258, 2009.
- [3] S. Xu, J. Ng, A. J. Du, J. Liu, and D. D. Sun, "Highly efficient TiO_2 nanotube photocatalyst for simultaneous hydrogen production and copper removal from water," *International Journal of hydrogen energy*, vol. 36, pp. 6538–6545, 2011.
- [4] C. Yu, D. Cai, K. Yang, J. C. Yu, Y. Zhou, and C. Fan, "WO₃ Coupled P-TiO₂ Photocatalysts with Mesoporous Structure," *J. Phys. Chem. Solids*, vol. 71, pp. 1337–1343, 2010.
- [5] R. L. Narayana, M. Matheswaran, A. A. Aziz, and P. Saravanan, "Photocatalytic decolorization of basic green dye by pure and Fe, Co doped TiO_2 under daylight illumination," *Desalination*, vol. 269, pp. 249–253, 2011.
- [6] J. C. Xu, Y. L. Shi, J. E. Huang, B. Wang, and H. L. Li, "Doping metal ions only onto the catalyst surface," *Journal of Molecular Catalysis A: Chemical*, vol. 219, pp. 351–355, 2004.
- [7] L. C. Chen, C. M. Huang, and F. R. Tsai, "Characterization and photocatalytic activity of K⁺-doped TiO_2 photocatalysts," *J. Mol. Catal. A: Chem.*, vol. 265, pp. 133–140, 2007.
- [8] S. Nahar, K. Hasegawa, and S. Kagaya, "Photocatalytic degradation of phenol by visible light-responsive iron-doped TiO_2 and spontaneous sedimentation of the TiO_2 particles," *Chemosphere*, vol. 65, pp. 1976–1982, 2006.
- [9] C. C. Pan and J. C. S. Wu, "Visible-light response Cr-doped TiO_2 -xN_x photocatalysts," *Mater. Chem. Phys.*, vol. 100, pp. 102–110, 2006.
- [10] J. Choi, H. Park, and M. R. Hoffmann, "Effects of Single Metal-Ion Doping on the Visible-Light Photoreactivity of TiO_2 ," *J. Phys. Chem. C*, vol. 114, pp. 783–792, 2010.
- [11] S. Mozia, M. Tomaszewska, B. Kosowska, B. Grzmil, A. W. Morawski, and K. Kalucki, "Decomposition of nonionic surfactant on a nitrogen-doped photocatalyst under visible-light irradiation," *Appl. Catal. B*, vol. 55, pp. 195, 2005.
- [12] H. Tokudome and M. Miyauchi, "N-doped TiO_2 Nanotube with Visible Light Activity," *Chem. Lett.*, vol. 33, pp. 1108, 2004.
- [13] R. Asapu, V. M. Palla, B. Wang, Z. Guo, R. Sadu, and D. H. Chen, "Phosphorus-doped titania nanotubes with enhanced photocatalytic

activity,” *Journal of Photochemistry and Photobiology A: Chemistry*, vol. 225, pp. 81–87, 2011.

- [14] H. N. Guan, D. F. Chi, J. Yu, and S. Y. Zhang, “Novel photodegradable insecticide W/TiO₂/Avermectin nanocomposites obtained by polyelectrolytes assembly,” *Colloid Surf. B: Biointerface*, vol. 83 pp. 148–154, 2011.
- [15] G. Colón, M. Maicu, M. C. Hidalgo, and J. A. Navío, “Cu-doped TiO₂ system with improved photocatalytic activity,” *Appl. Catal. B Environ.*, vol. 67, pp. 41–51, 2006.
- [16] K. Nagaveni, M. S. Hegde, and G. Madras, “Structure and photocatalytic activity of Ti_{1-x}M_xO₂ +/-delta (M = W, V, Ce, Zr, Fe, and Cu synthesized by solution combustion method,” *Phys. Chem. B*, vol. 108, pp. 20204 – 20212, 2004.
- [17] K. R. , P. A. Pulagurla, L. R. Venkata, M. S. Vutukuri, S. Basavaraju, D. K. Valluri, and S. Machiraju, “Photocatalytic Degradation of Isoproturon Pesticide on C, N and S Doped TiO₂,” *J. Water Resource and Protection*, vol. 2, pp. 235–244, 2010.
- [18] S. Slamet, W. N. Hosna, P. Ezza, K. Soleh, and G. Jarnuzi, “Photocatalytic reduction of CO₂ on copper-doped titania catalysts prepared by improved-impregnation method,” *Catalysis Communications*, vol. 6, pp. 313–319, 2005.
- [19] G. Liu, Z. G. Chen, C. L. Dong, Y. N. Zhao, F. Li, G. Q. Lu, and H. M. Cheng, “Visible Light Photocatalyst: Iodine-Doped Mesoporous Titania with a Bicrystalline Framework,” *J. Phys. Chem. B*, vol. 110, pp. 20823–20828, 2006.
- [20] H. Wang, Y. Wu, and B. Q. Xu, “Preparation and characterization of nanosized anatase TiO₂ cuboids for photocatalysis,” *Appl Catal B.*, vol. 5, no. 59, pp. 139–146, 2005.
- [21] I. Guy, A. Peigney, H. Andrianjatova, and A. Rousset, “Texture control of spherical undoped and Bi-doped zinc oxide powders,” *J. Mater. Process. Technol.* vol. 56, pp. 98–107, 1996.
- [22] C. D. Valentin, E. Finazzi, G. Pacchioni, A. Selloni, S. Livraghi, M. C. Paganini, and E. Giamello, “N-doped TiO₂: Theory and experiment,” *Chem. Phys.* vol. 339, no. 1-3, pp. 44–56, 2007.
- [23] V. Kumar, S. K. Sharma, T. P. Sharma, and V. Singh, “Band gap determination in thick films from reflectance measurements,” *Optical Materials*, vol. 12, pp. 115–119, 1999.



Mohd Hasmizam Razali is a Ph.D. candidate in Materials Engineering (Nanomaterials) at School of Materials and Mineral Resources Engineering, Universiti Sains Malaysia, Malaysia. He obtained his M.Sc. and Bachelors degree in Chemistry from Universiti Teknologi Malaysia, Malaysia in 2005 and 2003 respectively.

His research is currently focused on designing the functional nanomaterials and heterogeneous catalysis, which are useful in converting various forms of energy and also in reducing environmental pollution.



Ahmad-Fauzi M. N. received his Bachelor degree in Applied Sc. from Universiti Sains Malaysia, Malaysia in 1985. He subsequently obtained his M.Sc. from University of Leeds, UK in 1987 and Ph.D. degree in ceramics from University of Sheffield, UK in 1995

He is currently a professor at School of Materials and Mineral Resources Engineering, Universiti Sains Malaysia. He has published more than 50 international

journal articles. His research interests are in the areas of ceramics, composites materials and nanomaterials for semiconducting materials and environmental.



Abdul Rahman Mohamed received his chemical engineering degree from University of Southern California, USA. He subsequently obtained his M. Sc. and Ph.D. degree in chemical engineering from University of Hampshire, USA. He is an internationally recognized expert in the field of nanoscience and nanotechnology and currently is a professor at School of Chemical Engineering, Universiti Sains Malaysia. His research

spans the areas of reaction engineering and catalysis, biofuel technology, air pollution and wastewater monitoring and control.



Srimala Sreekantan obtained her Ph.D. from Universiti Sains Malaysia, Malaysia. She currently serves as an associated professor who is holding the senior lecturer position at the School of Material and Mineral Resources Engineering, University Sains Malaysia, Malaysia. Her research interests are based on nanostructured material.